

Bias-induced local heating in atom-sized metal contacts at 77 K

Makusu Tsutsui,^{a)} Shu Kurokawa, and Akira Sakai

International Innovation Center, Kyoto University, Sakyo-ku, Kyoto 606-8501, Japan

(Received 17 January 2007; accepted 4 March 2007; published online 30 March 2007)

Local heating in Zn atom-sized contacts is studied at 77 K under high biases. Switching rate ν of two-level fluctuations of the contact conductance is measured and statistically analyzed to estimate the contact effective temperature. Typical $\log \nu$ increases linearly with the bias up to 0.35 V, which suggests negligible contact heating in the low-bias regime. Above 0.4 V, however, $\log \nu$ rises steeply with the bias due to an onset of contact overheating. The estimated contact temperature rises more rapidly with the bias than the \sqrt{V} dependence derived theoretically. © 2007 American Institute of Physics. [DOI: 10.1063/1.2719682]

One of the important issues toward practical realizations of atomic and molecular electronics is local contact heating under high-bias/current conditions. The local heating of atomic and molecular contacts has thus been a subject of intensive studies in recent years.^{1–11} Theoretical investigations^{1–3} have indicated that the contact cooling, i.e., heat diffusion away from the contact via lattice thermal conduction, effectively alleviates the heating effects, and, by assuming bulk thermal conduction mechanism, the contact temperature is derived as

$$T_{\text{eff}} = (T_V^4 + T_0^4)^{1/4}, \quad (1)$$

$$T_V = \gamma\sqrt{LV}, \quad (2)$$

where T_0 is the ambient temperature, T_V is the bias-dependent temperature, and L and γ are the contact length and a material-dependent parameter, respectively.^{1,2} The theoretical model has been applied to discuss not only local heating in atom-sized contacts (ASCs) of metals at 4 K (Refs. 8 and 11) but also high-bias heating in single molecular junctions at room temperature.⁴ However, the derivation of T_{eff} in Eqs. (1) and (2) assumes T^3 law for heat capacity of the contact, the approximation of which is applicable only at low ambient temperatures satisfying $T_0/\Theta \ll 1$, with Θ being the Debye temperature. Therefore, validity of the theoretical $T_{\text{eff}}-V$ relation at T_0 's well above 4 K is by no means a trivial assumption. On the other hand, since performances of ASCs at $T_0 > 4$ K are more relevant to device applications than at 4 K, elucidation of the local heating in metal ASCs at higher T_0 is an important issue from a practical viewpoint.

It has been demonstrated previously that T_{eff} of Au and Cu ASCs shows negligible increase in T_{eff} in a bias range $V \leq 0.60$ V.^{9,10} The absence of the overheating in Au ASCs at 77 K, together with the existence at 4 K,¹¹ suggests that the contact cooling is more effective at 77 K than at 4 K, in accordance with the theoretical heat dissipation via the lattice heat conduction.² Furthermore, it was observed that T_{eff} of Ag ASCs starts to increase at 0.5 V at which Au and Cu ASCs show no sign of overheating. The result suggests that not only Θ but also the melting point T_m of metals is an important factor that characterizes the contact local heating, since Ag has lower T_m than Cu and Au but higher Θ than Au. To gain deeper insight on the material dependence of the

local contact heating, T_{eff} of Zn ASCs is studied at 77 K. Zn possesses even lower T_m than Ag, while Θ is comparable to that of Cu. Experiments on T_{eff} of Zn ASCs are thus expected to clarify which would be the relevant material parameter for the overheating of metal ASCs.

Frequency of two-level fluctuations (TLFs) of contact conductance is measured in order to estimate the T_{eff} of Zn ASCs. The conductance TLF originates from jumps of contact atoms between two distinct positions. The atomic jump is a thermally activated process and leads to the conductance TLF with a frequency ν expressed as

$$\nu = \nu_0 \exp[-(E_B - \zeta V)/k_B T_{\text{eff}}], \quad (3)$$

where ν_0 and E_B are an attempt frequency and an energy barrier against the jump, respectively, and the parameter ζ characterizes the bias-current-induced barrier reduction. A conventional scheme to determine T_{eff} is to hold a TLF state and meanwhile sweep the bias while measuring changes in $\ln \nu$.^{6,7} However, the method is not applicable at 77 K where each TLF state is too short lived to conduct neither the bias sweep nor a reliable frequency measurement. Thus, we have developed an alternative “statistical” approach,^{9–11} where ν of a large number of TLF states are measured and summarized in the form of histogram, from which a peak frequency ν_m of the frequency distribution is extracted and T_{eff} is derived by examining the bias sensitivity of $\ln \nu_m$.

Zn ASCs were formed by utilizing the mechanically controllable break junction technique, the details of which are described elsewhere.¹² By manipulating the substrate bending, a Zn wire (99.999%) is mechanically broken at 77 K and subsequently fine adjusted to obtain a junction that exhibits a TLF switching while monitoring the conductance with an oscilloscope. The data recorded were only those demonstrating a two-level switching within a conductance window of $(2-3)G_0$, which corresponds to contact sizes of two to four atoms,^{13,14} stably throughout the time range of the oscilloscope. A typical conductance trace showing the TLF between $2.4G_0$ and $2.7G_0$ is displayed in Fig. 1. Since the TLF frequency changes for orders of magnitudes with the bias, the recording time window was varied accordingly from 5 to 500 ms in order to maintain an equal statistical accuracy in the frequency measurements at different biases. The bias is set from 0.20 to 0.45 V with a 0.05 V step, and 100 TLF traces were acquired at each bias. Every time after recording one TLF trace, the contact is closed to $>10G_0$ for eliminating possible history effects.

^{a)}Electronic mail: makusu32@sanken.osaka-u.ac.jp

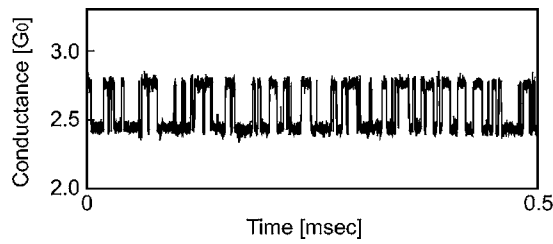


FIG. 1. Typical TLF trace obtained at 0.35 V.

Figure 2 displays the histograms of ν . Note that the frequency is taken in a logarithmic scale. As is evident from the figure, ν covers a wide range spanning over more than five orders of magnitudes. The broad frequency distribution is not unexpected considering a diversity in the contact configuration and the resulting variation of E_B in Eq. (3). A distribution of $\Delta E_B \sim 0.1$ eV is sufficient to account for the observed range of ν . Since E_B typically varies ~ 0.1 – 1.0 eV for different ASC configurations,¹⁵ the orders-of-magnitude diversity in ν is acceptable.

The histograms represent a single-peak profile that apparently shifts to higher frequencies with increasing the bias. To quantitatively examine the bias dependence of ν , a peak frequency ν_m is extracted by fitting each profile to a Gaussian distribution. Figure 3(a) depicts a plot of $\log \nu_m$ with respect to the bias. Up to 0.35 V, $\log \nu_m$ increases linearly as $\log \nu_m \propto V$. Assuming that ν_m varies with V according to Eq. (3), the observed proportionality between $\log \nu_m$ and V indicates that T_{eff} remains unchanged with the bias, i.e., $T_{\text{eff}} \sim T_0 = 77$ K. Thus, there occurs no contact heating at $V \leq 0.35$ V. All the features of the TLF frequency distribution and ν_m presented in the figures are in good agreement with those reported for noble metal ASCs.^{9,10} From the slope of the $\log \nu_m$ - V plot in Fig. 3(a), we can estimate ζ in Eq. (3) as 0.14 eV/V with $T_{\text{eff}} = 77$ K. Table I tabulates experimental values of ζ of Zn and noble metal ASCs. As seen in the table, ζ_{Zn} is comparable to ζ 's of noble metals but $\sim (25\text{--}75)\%$

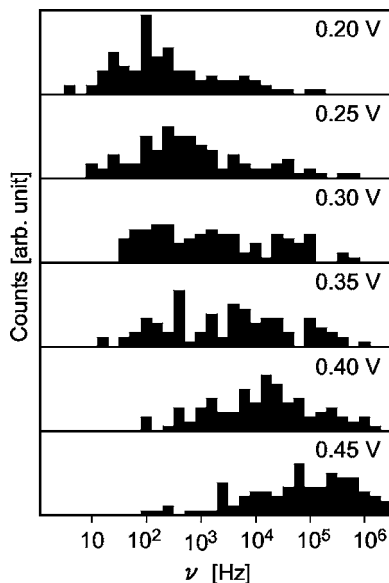


FIG. 2. Histograms constructed based on 100 TLF traces obtained at a constant bias. Note that ν widely distributes for more than five orders of magnitude. Furthermore, each histogram shows a single pronounced peak, from which a main peak frequency ν_m is extracted by fitting a Gaussian distribution to each histogram.

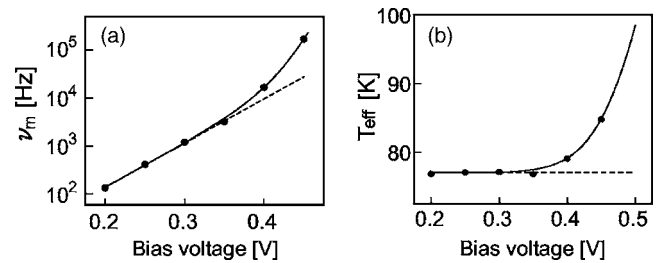


FIG. 3. (a) Semilogarithmic plot of ν_m with respect to the bias. $\log \nu_m$ scales linearly with the bias at ≤ 0.35 V, which suggests $T_{\text{eff}} \sim T_0 = 77$ K over the bias range. Above 0.40 V, in contrast, ν_m increases rapidly with the bias. The transition in the $\log \nu_m$ - V dependence signifies an onset of the contact overheating, giving rise to rapid increase in T_{eff} above the ambient temperature. The solid curve is a fit to the plot with Eq. (3) assuming $T_V = \alpha V^3$. (b) The bias dependence of T_{eff} deduced from the $\log \nu_m$ - V plot. The solid curve is a fit to the plot with $T_V = \alpha V^3$.

higher. ASCs of higher ζ are more susceptible to bias-/current-induced forces and would be more unstable at high biases. The observed higher ζ_{Zn} is thus compatible with the lower critical current density for the contact break of Zn ASCs.¹⁶

Above 0.35 V, $\log \nu_m$ starts to deviate from the linear bias dependence and rises steeply with the bias. The threshold bias for the sharp upturn of ν_m is denoted by V_{th} . Experimental values of V_{th} are compared in Table I for Zn and noble metal ASCs. Note that Zn ASCs show the lowest V_{th} . Two possible mechanisms can be considered responsible for the high-bias $\log \nu_m$: current-induced forces and contact overheating. The current-induced forces acting on contact atoms become prominent at high biases and would reach the breakup strength of the ASCs,¹⁷ leading to the sharp rise in $\log \nu_m$. They, however, appear to make little influence on the TLF of Au ASCs up to 1 V,¹¹ at which the forces are estimated to approach the contact breaking value.¹⁸ Therefore, although the response of Zn ASCs to the current-induced forces might be different from that of Au ASCs, the appreciable high-bias ν_m increment observed in the present study is likely to be caused mainly by contact overheating rather than the current-induced forces.

Thus, the observed sharp increase in $\log \nu_m$ signifies an onset of contact overheating, i.e., $T_{\text{eff}} > T_0$. To understand the material dependence of V_{th} , we first point out that the deviation of T_{eff} from T_0 becomes noticeable only when T_V in Eq. (1) becomes $T_V > T_0$. Thus, at $V = V_{\text{th}}$, $T_{V_{\text{th}}} = \gamma \sqrt{L V_{\text{th}}} \sim T_0$, or $V_{\text{th}} \sim (T_0 / \gamma)^2 / L$. This shows that the material dependence of V_{th} comes through γ . According to the theoretical model by Todorov,¹ γ contains two material-dependent temperatures, Debye temperature Θ and melting point T_m , characterizing the lattice cooling efficiency and the inelastic electron mean free path, respectively. Higher Θ (i.e., lower thermal cooling) and/or lower T_m (i.e., shorter mean free path) yields larger γ . Since Zn possesses higher Θ and lower T_m than Au

TABLE I. Parameters of the conductance TLF of Zn and noble metal ASCs.

Metal	Θ (K)	T_m (K)	ζ (eV/V)	V_{th} (V)	Ref.
Au	165	1338	0.08	>0.6	10
Cu	343	1358	0.11	>0.6	10
Ag	225	1235	0.11	0.5	10
Zn	327	693	0.14	0.4	This work

and Ag, the observed lower V_{th} of Zn is consistent with the theoretical γ . However, Cu shows the highest V_{th} though Θ is comparable to that of Zn. It is thus likely that T_m , rather than Θ , plays a predominant role in the material dependence of V_{th} . The negative correlation between V_{th} and T_m suggests that the inelastic electron mean free path should be the relevant parameter for determining the material-dependent overheating in metal ASCs at 77 K. The dependence of V_{th} on Θ would emerge at lower temperatures, where the lattice thermal cooling becomes more crucial.

Finally, T_{eff} is estimated from the measured bias dependence of ν_m . First, we obtain $\zeta \sim 0.14$ eV/V and $E_B \sim 0.19$ eV from the linear part of the $\log \nu_m$ - V plot in Fig. 3(a), assuming $\nu_0 \sim 10^{13}$ Hz. Substituting the parameters into Eq. (3), T_{eff} is calculated from ν_m . The result is displayed in Fig. 3(b). Below $V_{th}=0.4$ V, T_{eff} agrees with $T_0=77$ K as expected, while it rapidly increases for $V > V_{th}$ and reaches ~ 85 K at 0.45 V. We attempted to describe the observed T_{eff} - V curve by Eq. (1) by assuming an appropriate bias dependence for T_V . We applied a power-law behavior $T_V = \alpha V^\beta$ and obtained the best result with $\beta=3$. Solid curves in Figs. 3(a) and 3(b) represent the result of the fitting. Smaller exponents such as $\beta=1/2$, which has been theoretically predicted¹ and experimentally verified for Au ASCs at 4.2 K,¹¹ cannot well reproduce the sharp temperature rise for $V > V_{th}$. Thus, the contact overheating grows up with the bias more rapidly at 77 K than at 4.2 K. At present, however, the physics underlying the rapid contact heating is unclear. It is only speculated that at high ambient temperature conditions, many phonon modes are excited and simultaneously larger proportion of phonon-phonon scattering will cause phonon momentum changes, giving rise to additional thermal resistance. As a result, the cooling through the lattice heat conduction, which tends to suppress T_{eff} at higher biases, becomes less efficient at 77 K than at 4.2 K.

In summary, we have studied the bias-induced local heating in Zn ASCs at 77 K through measuring the conductance TLF frequency. The bias dependence of ν is analyzed by examining bias shifts of the peak frequency ν_m extracted

from the frequency histograms. The onset of the bias-induced contact overheating is detected by observing the rapid and nonlinear increase in the $\log \nu_m$ - V plot. The threshold bias for Zn ASCs is $V_{th}=0.4$ V, which is lower than that of noble metal ASCs. The negative correlation between V_{th} and the melting point of metals suggests that, instead of the lattice conduction, the inelastic electron mean free path, characterized by the melting point, effectively affects the contact local heating in ASCs at 77 K.

¹T. N. Todorov, *Philos. Mag. B* **77**, 965 (1997).

²T. N. Todorov, J. Hoekstra, and A. P. Sutton, *Phys. Rev. Lett.* **86**, 3606 (2001).

³Y.-C. Chen, M. Zwolak, and M. Di Ventra, *Nano Lett.* **3**, 1691 (2003).

⁴Z. Huang, B. Xu, Y. Chen, M. Di Ventra, and N. Tao, *Nano Lett.* **6**, 1240 (2006).

⁵R. D'Agosta, N. Sai, and M. Di Ventra, *Nano Lett.* **6**, 2935 (2006).

⁶H. E. van den Brom, A. I. Yanson, and J. M. van Ruitenbeek, *Physica B* **252**, 69 (1998).

⁷H. E. van den Brom, Y. Noat, and J. M. van Ruitenbeek, in *Kondo Effect and Dephasing in Low-Dimensional Metallic Systems*, edited by V. Chandrasekhar, C. van Haesendonck, and A. Zawadowski (Kluwer Academic, Dordrecht, 2001), p. 249.

⁸R. H. M. Smit, C. Untiedt, and J. M. van Ruitenbeek, *Nanotechnology* **15**, S472 (2004).

⁹M. Tsutsui, Y. Taninouchi, S. Kurokawa, and A. Sakai, *Jpn. J. Appl. Phys., Part 1* **44**, 5188 (2005).

¹⁰M. Tsutsui, Y. Teramae, S. Kurokawa, and A. Sakai, *Appl. Surf. Sci.* **252**, 8677 (2006).

¹¹M. Tsutsui, S. Kurokawa, and A. Sakai, *Nanotechnology* **17**, 5334 (2006).

¹²N. Agrait, A. L. Yeyati, and J. M. van Ruitenbeek, *Phys. Rep.* **377**, 81 (2003).

¹³P. Konrad, C. Bacca, E. Scheer, P. Brenner, A. Mayer-Gindner, and H. v. Löhneysen, *Appl. Phys. Lett.* **86**, 213115 (2005).

¹⁴E. Scheer, P. Konrad, C. Bacca, A. Mayer-Gindner, H. v. Löhneysen, M. Häfner, and J. C. Cuevas, *Phys. Rev. B* **74**, 205430 (2006).

¹⁵M. R. Sørensen, K. W. Jacobsen, and H. Johnson, *Phys. Rev. Lett.* **77**, 5067 (1996).

¹⁶R. Suzuki, Y. Mukai, M. Tsutsui, S. Kurokawa, and A. Sakai, *Jpn. J. Appl. Phys., Part 1* **45**, 7217 (2006).

¹⁷Z. Yang, M. Chshiev, M. Zwolak, Y.-C. Chen, and M. Di Ventra, *Phys. Rev. B* **71**, 041402 (2005).

¹⁸M. Brandbyge, K. Stokbro, J. Taylor, J.-L. Mozos, and P. Ordejon, *Phys. Rev. B* **67**, 193104 (2003).